Journal of the Mechanics and Physics of Solids 58 (2010) 1088–1099

Contents lists available at ScienceDirect

Journal of the Mechanics and Physics of Solids

journal homepage: www.elsevier.com/locate/jmps

Special rotational deformation as a toughening mechanism in nanocrystalline solids

N.F. Morozov [a], I.A. Ovid'ko [a,1], A.G. Sheinerman [a,*], E.C. Aifantis [b]

[a] Institute of Problems of Mechanical Engineering, Russian Academy of Sciences, Bolshoj 61, Vasil. Ostrov, St. Petersburg 199178, Russia
[b] Aristotle University of Thessaloniki, 54124 Thessaloniki, Greece

ARTICLE INFO

Article history:
Received 29 May 2009
Received in revised form
20 October 2009
Accepted 12 April 2010

Keywords:
Nanocrystalline materials
Cracks
Rotational deformation

ABSTRACT

A theoretical model is suggested which describes the effect of special rotational deformation on crack growth in deformed nanocrystalline ceramics and metals. Within the model, the special rotational deformation (driven by the external stress concentrated near the tip of a mode I crack) occurs in a nanograin through formation of immobile disclinations whose strengths gradually increase during the formation process conducted by grain boundary sliding and diffusion. The special rotational deformation releases, in part, local stresses near the crack tip, thus serving as a toughening mechanism in nanocrystalline materials. The effects of the special rotational deformation on the growth of pre-existent, comparatively large cracks in nanocrystalline metals and ceramics are estimated.

1. Introduction

Nanocrystalline metallic and ceramic materials show outstanding mechanical properties (superstrength, superhardness, good wear resistance) and represent the subject of intensive research efforts (see e.g., Kuntz et al., 2004; Wei and Anand, 2004; Ovid'ko, 2005; Pande and Masumura, 2005; Wolf et al., 2005; Capolungo et al., 2007; Dao et al., 2005; Koch et al., 2007; Mukhopadhyay and Basu, 2007; Tomar and Zhou, 2007; Barai and Weng, 2008a, 2008b; Choi et al., 2008; Gurtin and Anand, 2008; Wei and Hao, 2008; Wei et al., 2008; Aifantis, 2009; Morozov et al., 2009; Pande and Cooper, 2009; Weng, 2009; Yang and Yang, 2009). However, in most cases, nanocrystalline materials exhibit both low tensile ductility and low fracture toughness, which considerably limit their practical utility; see e.g., reviews (Kuntz et al., 2004; Ovid'ko, 2005; Wolf et al., 2005; Dao et al., 2005; Mukhopadhyay and Basu, 2007) and book (Koch et al., 2007). These mechanical properties of nanocrystalline materials are caused by their structural features, first of all, by nanoscale grain sizes and large amounts of grain boundaries. In particular, grain boundaries significantly or even completely suppress the lattice dislocation slip in nanocrystalline materials and cause the effective action of alternative deformation modes conducted by grain boundaries (see e.g., Ovid'ko, 2005; Wolf et al., 2005; Dao et al., 2005; Koch et al., 2007). This is contrasted to conventional coarse-grained polycrystals, where grain boundaries influence the lattice dislocation slip (see e.g., Aifantis et al., 2005, 2006; Aifantis and Ngan, 2007), but their effect is not so dramatic, and the lattice slip commonly plays the role of the dominant deformation mode.

Despite the fact that most nanocrystalline materials have low tensile ductility and low fracture toughness, there are intriguing examples of nanocrystalline materials showing good tensile ductility and/or enhanced toughness

* Corresponding author.
E-mail addresses: ovidko@def.ipme.ru (I.A. Ovid'ko), shein77@mail.ru (A.G. Sheinerman).
[1] Tel.: +7 812 321 4764; fax: +7 812 321 4771.

0022-5096/$ - see front matter © 2010 Elsevier Ltd. All rights reserved.
doi:10.1016/j.jmps.2010.04.003

characteristics. For instance, several research groups reported on toughness enhancement of single-phase and composite nanocrystalline materials, compared to that of their coarse-grained polycrystalline or single-crystalline counterparts, in which case the reduction in the grain size plays the dominant role in toughness enhancement (Bhaduri and Bhaduri, 1997; Mirshams et al., 2001; Zhao et al., 2004; Kaminskii et al., 2005; Pei et al., 2005; Koch et al., 2007). (Also, there are situations where nanocrystalline composites show enhanced toughness characteristics, due to other factors associated with the presence of second-phase nanoparticles or carbon nanotubes (Siegel et al., 2001; Zhan et al., 2003; Kuntz et al., 2004; Liu et al., 2008).) With these examples and the specific structural features of nanocrystalline materials, one expects that there are toughening mechanisms that intensively operate in these materials, but are not effective in conventional polycrystalline materials. In this context, from both fundamental and applied viewpoints, there is a large interest in understanding the toughening mechanisms that are specific for nanocrystalline materials. Recently, creep deformation conducted by grain boundary processes [Ashby–Verall creep carried by intergrain sliding accommodated by grain boundary diffusion and grain rotations (Ashby and Verall, 1973; Yang and Wang, 2004)] has been suggested as a toughening micromechanism inherent to nanocrystalline metals (Yang and Yang, 2008, 2009). Besides, nanoscale deformation twinning (Gutkin et al., 2008) and stress-driven migration of grain boundaries (Ovid'ko et al., 2008) have been theoretically described as specific toughening mechanisms for nanocrystalline metals and ceramics. Following experimental data (Chen et al., 2003; Jin et al., 2004; Soer et al., 2004; De Hosson et al., 2006; Zhang et al., 2004, 2005; Liao et al., 2004; Wang et al., 2005), both nanoscale deformation twinning and stress-driven migration of grain boundaries can also serve as specific deformation modes operating in nanocrystalline materials. That is, specific toughening mechanisms can be attributed to specific deformation modes in nanocrystalline materials. In this context, in the light of the experimentally documented fact (Milligan et al., 1993; Ke et al., 1995; Hackney et al., 1996; Mukherjee, 2002; Murayama et al., 2002; Shan et al., 2004; Zizak et al., 2008) that rotational deformation (plastic deformation accompanied by crystal lattice rotations) often occurs in nanocrystalline materials, one naturally expects rotational deformation to contribute to toughening of such materials.

Rotational deformation by definition represents plastic deformation accompanied by crystal lattice rotations in deformed grains of conventional coarse-grained polycrystals (Romanov and Vladimirov, 1992) and nanocrystalline materials (Ovid'ko, 2002; Gutkin and Ovid'ko, 2004). The first group which seems to have documented the critical role of grain boundary dislocation processes in nanocrystalline materials, leading to grain rotation/sliding, is that of Aifantis and co-workers (Milligan et al., 1993; Ke et al., 1995; Hackney et al., 1996; see also the reviews by Aifantis (2000, 2009)). Their work on in-situ TEM observations of plastically deforming gold and silver nanograin films (grain diameter less than 8–10 nm) revealed the absence of bulk dislocation activity; instead, nanopore nucleation and growth at triple grain boundary junctions were observed, followed by void coalescence and nanodamage development. In addition, large grain rotations (5–7°, up to 15°) were observed and the strain tensor was measured inside the microscope by an in-situ strain nanorosette giving an estimate for the effective plastic strain up to 30–35%. Some initial mechanics models were also suggested to interpret these observations. In recent years, the representations on rotational deformation in nanocrystalline materials have been intensively developed. In particular, experiments (Mukherjee, 2002; Murayama et al., 2002; Shan et al., 2004), computer simulations (Latapie and Farkas, 2004; Shimokawa et al., 2005; Szlufarska et al., 2005) and theoretical models (Gutkin et al., 2003; Gutkin and Ovid'ko, 2004; Joshi and Ramesh, 2008; Ovid'ko and Sheinerman, 2008; Bobylev et al., 2009a) have provided convincing evidence for the important role of rotational deformation in plastic flow processes in various nanocrystalline materials.

In general, one can distinguish standard and special rotational deformation modes carried by mobile and immobile disclinations, respectively. Following Romanov and Vladimirov (1992), an elemental act of standard rotational deformation is the movement of a dipole of wedge disclinations with constant strengths $\pm\omega$ (Fig. 1a–e). Within this standard view, the movement of disclination dipoles in nanocrystalline materials is associated with such structural transformations as absorption of lattice dislocations from grain interior regions (Romanov and Vladimirov, 1992) (Fig. 1b–e), lattice dislocation emission from grain boundaries (Gutkin et al., 2002a) or grain boundary migration (Gutkin and Ovid'ko, 2005; Ovid'ko et al., 2008). The special rotational deformation occurs in a nanograin through the formation of immobile disclinations located at nanograin boundary junctions, and this deformation mode is specified by a gradual increase of strengths of the immobile disclinations during their formation process conducted by grain boundary sliding and diffusion (Ovid'ko and Sheinerman, 2008) (Fig. 1a, f–i). Standard rotational deformation through movement of disclination dipoles was previously considered as that occurring near crack tips and hampering crack growth (Romanov and Vladimirov, 1992; Ovid'ko et al., 2008). In this paper, we consider the hampering effect of the special rotational deformation (Fig. 1f–i) [which can effectively operate in nanocrystalline materials, but is commonly suppressed in coarse-grained polycrystals (Ovid'ko and Sheinerman, 2008)] on crack growth in nanocrystalline materials.

2. Effects of disclination quadrupole produced by special rotational deformation on fracture toughness of nanocrystalline solids: theoretical model and estimates

Let us consider a deformed nanocrystalline specimen under a tensile load (external stress) σ_0. The specimen is assumed to be an elastically isotropic solid having the shear modulus G and Poisson's ratio ν. Let a long flat crack develop under the action of the applied load in the solid (Fig. 2). The crack is assumed to propagate perpendicularly to the direction of the

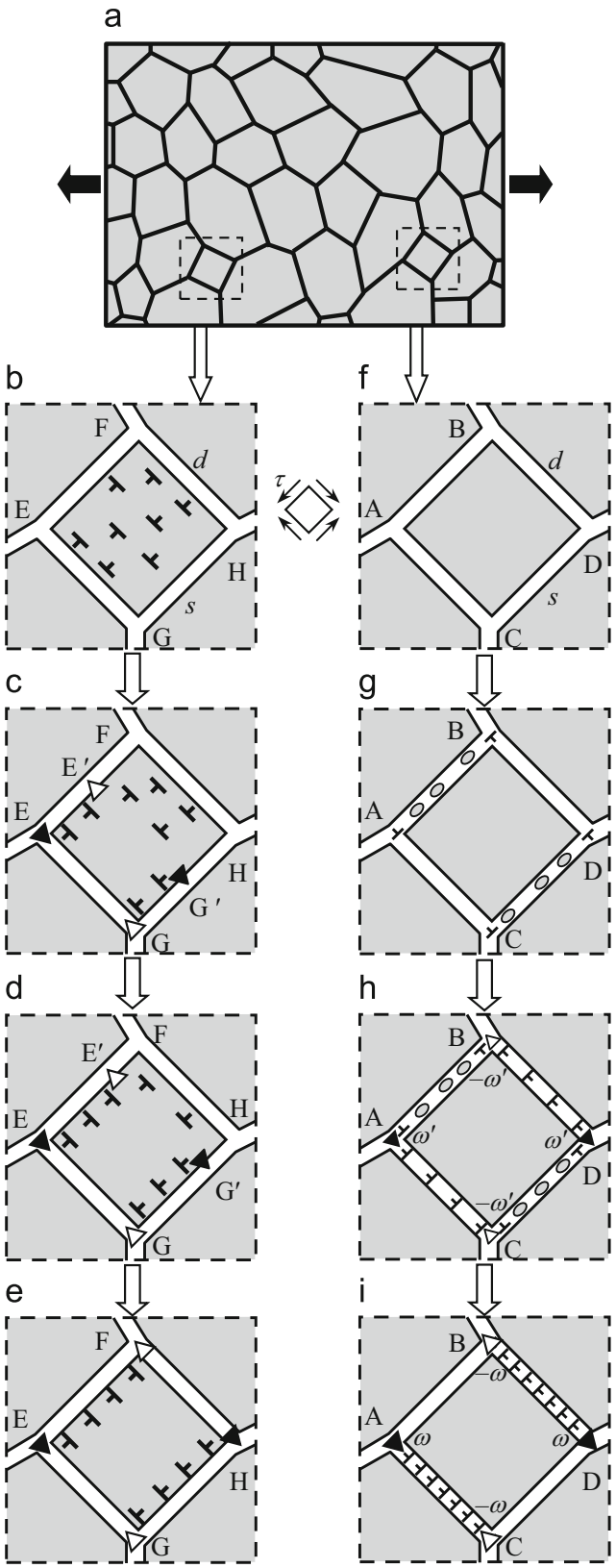

Fig. 1. Rotational deformation modes in model square grains of a nanocrystalline specimen (schematically). (a) Tensile deformation of a nanocrystalline specimen. General view. (b)–(e) Standard rotational deformation is carried by mobile disclinations (triangles). A quadrupole of disclinations at points E, E', G and G' is formed. The disclinations at points E and G are immobile, while the disclinations at points E' and G' move along grain boundaries EF and GH through absorption of lattice dislocations from grain interior. These moving disclinations carry rotational deformation. (f)–(i) Special rotational deformation occurs in a nanograin through formation of immobile disclinations (triangles), whose strengths gradually increase during the formation process conducted by grain boundary sliding and diffusion-controlled climb of grain boundary dislocations. Grain boundary sliding occurs through local shear events (grey ellipses) in grain boundaries AB and CD. Grain boundary sliding results in formation of grain boundary dislocations at junctions A, B, C and D. Diffusion-controlled climb of the dislocations along grain boundaries AC and BD provides special rotational deformation accompanied by formation and evolution of a quadrupole of wedge disclinations at junctions A, B, C and D.

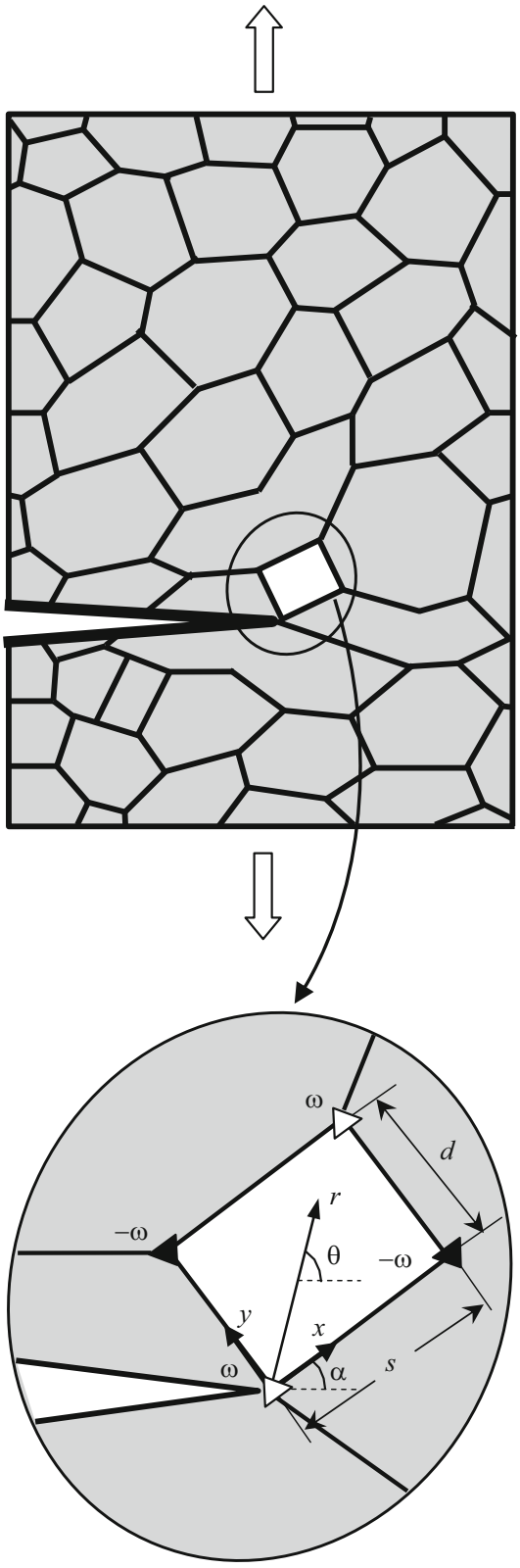

Fig. 2. Special rotational deformation in a deformed nanocrystalline specimen containing a mode I crack: (a) general view and (b) the magnified inset highlights a disclination quadrupole near the crack tip.

applied load (Fig. 2). That is, the crack is a mode I crack. Also, for simplicity, we restrict our consideration to a two-dimensional grain structure (that serves as a good model for columnar nanoscale structures of films and a first-approximation model for bulk nanocrystalline materials). This is related to the following three reasons: first, the analysis of real three-dimensional defect configurations in real nanoscale grains requires the knowledge of too many factors and

parameters, which can hardly be taken into an analytical consideration. Second, plastic deformation mechanisms are directly identified by ("in situ") transmission electron microscopy experiments, which commonly deal with nanocrystalline films having 2D-like columnar structures. In particular, rotational deformation – plastic deformation accompanied by crystal lattice rotations in nanoscale grains – was experimentally observed precisely in nanocrystalline films (see e.g., Milligan et al., 1993; Ke et al., 1995; Hackney et al., 1996; Shan et al., 2004). Third, numerous experiments showed high similarity between the deformation behaviors of nanocrystalline bulk materials and films; see e.g., the book by Koch et al. (2007) and references therein.

High stresses operating in deformed nanocrystalline solids and stress concentration near the crack tips can initiate the special rotational deformation of grains (Fig. 2). In the framework of the two-dimensional model, let us consider the special rotational deformation of a rectangular grain and the crack whose tip reaches a junction of boundaries of this grain, as shown in Fig. 2. In terms of the theory of defects, the special rotational deformation in such a grain can be described as the formation of a quadrupole of immobile wedge disclinations, whose strengths gradually grow during the formation process (Ovid'ko and Sheinerman, 2008) (Fig. 2). The special rotational deformation is conducted by grain boundary sliding along grain boundaries AB and CD and diffusion-controlled climb of grain boundary dislocations along grain boundaries AC and BD (Fig. 1f–i). Following the concept on local shear events – shear transformations of local atomic clusters – as carriers of plastic flow in grain boundaries in metals (Conrad and Narayan, 2000; Padmanabhan and Gleiter, 2004) and covalent solids (Demkowicz et al., 2007), we suppose that local shear events carry sliding along grain boundaries AB and CD. The sliding results in the formation of grain boundary dislocations at junctions A, B, C and D (see e.g., Bobylev et al., 2006, 2009b), as schematically shown in Fig. 1(f–i). Diffusion-controlled climb of the dislocations along grain boundaries AC and BD provides special rotational deformation accompanied by formation of quadrupole of wedge disclinations at grain boundary junctions A, B, C and D (Fig. 1f–i); for details, see Ovid'ko and Sheinerman (2008). The disclination quadrupole creates stresses that influence crack growth.

Let us consider the effect of disclination quadrupole produced due to special rotational deformation on fracture toughness of a nanocrystalline solid. To do so, we will use the standard crack growth criterion (Irwin, 1957) based on the balance between the driving force related to a decrease in the elastic energy and the hampering force related to occurrence of a new free surface during crack growth. In the examined case of the plane strain state, this criterion is given as (Irwin, 1957)

$$\frac{1-\nu}{2G}(K_I{}^2+K_{II}{}^2)=2\gamma_e, \tag{1}$$

where K_I and K_{II} are the intensity factors for normal (to crack line) and shear stresses, respectively; and γ_e is the effective specific surface energy. Here, we put $\gamma_e=\gamma$ (where γ is the specific surface energy) for the crack propagating inside a grain, and $\gamma_e=\gamma-\gamma_b/2$ (where γ_b is the specific grain boundary energy) for the crack that advances along a grain boundary. In the considered situation, where the crack growth direction is perpendicular to the direction of the external load, the coefficients K_I and K_{II} are given as

$$K_I=K_I^\sigma+k_I^q, \quad K_{II}=k_{II}^q. \tag{2}$$

Here, K_I^σ is the stress intensity factor induced by the applied load σ_0, while k_I^q and k_{II}^q are the intensity factors for the stresses created by the disclination quadrupole located near the crack tip (Fig. 2).

Within the macroscopic mechanical description, the effect of the local plastic flow – the special rotational deformation resulting in the formation of a disclination quadrupole – on crack growth can be accounted for through the introduction of the critical stress intensity factor K_{IC}. In this case, the crack is considered as propagating under the action of the tensile load perpendicular to the crack growth direction, while the presence of the disclination quadrupole simply changes the value of K_{IC} compared to the case of brittle crack propagation. In these circumstances, the critical condition for the crack growth can be represented as (see e.g., Panasyuk, 1988): $K_I^\sigma=K_{IC}$.

With expression (2) substituted to formula (1) and the critical condition $K_I^\sigma=K_{IC}$ taken into account, one finds the following expression for K_{IC}:

$$K_{IC}=\sqrt{(K_{IC}^\sigma)^2-(k_{IIC}^q)^2}-k_{IC}^q. \tag{3}$$

In formula (3), $K_{IC}^\sigma=\sqrt{4G\gamma_e/(1-\nu)}$ is the fracture toughness in the disclination-free case (i.e., the case of brittle fracture with the special rotational deformation being completely suppressed), $k_{IIC}^q=k_{II}^q|_{K_I^\sigma=K_{IC}}$ and $k_{IC}^q=k_I^q|_{K_I^\sigma=K_{IC}}$. It should be noted that the quantities k_{IIC}^q and k_{IC}^q depend on K_{IC}, and so formula (3) represents an equation for the determination of K_{IC}. In order to characterize the effect of the disclination quadrupole produced by the special rotational deformation (Fig. 1) on crack growth, one should compare the critical stress intensity factor K_{IC} with the quantity K_{IC}^σ.

Let us calculate the critical stress intensity factor K_{IC} in the situation, where the disclination quadrupole forms near the crack, as shown in Fig. 2. We denote the disclination strengths as $\pm\omega$, the quadrupole arms as s and d, and the angle between the crack plane and one of the quadrupole arms as α (see Fig. 2). We also introduce a Cartesian coordinate system (x, y) and a polar coordinate system (r, θ) with the origin at the crack tip (see Fig. 2). The quadrupole arms are assumed to be small compared to the crack length l ($s, d \ll l$). This assumption allows us to model the crack as a semi-infinite one in the calculation of the stress intensity factors k_I^q and k_{II}^q. (In the limit of a semi-infinite crack, the disclination ω at the crack tip becomes located at an external free surface and disappears, in which case the disclination quadrupole transforms into three disclinations.) The stress intensity factors for the disclination quadrupole shown in Fig. 2 are calculated using the known expressions (Lin and Thompson,

1986; Zhang and Li, 1991) for the stress intensity factors of an edge dislocation near the tip of a semi-infinite crack. This is done through the standard representation (Romanov and Vladimirov, 1992) of disclination dipoles as continuous distributions of edge dislocations. As a result, we obtain $k_I^q = G\omega\sqrt{d}f_1(\alpha,t)/[2\sqrt{2\pi}(1-\nu)]$, $k_{II}^q = G\omega\sqrt{d}f_2(\alpha,t)/[2\sqrt{2\pi}(1-\nu)]$, where $t=s/d$,

$$f_1(\alpha,t) = \sum_{k=1}^{3} (-1)^k \sqrt{\tilde{r}_k}[3\cos(\theta_k/2)+\cos(3\theta_k/2)],$$

$$f_2(\alpha,t) = \sum_{k=1}^{3} (-1)^k \sqrt{\tilde{r}_k}[\sin(\theta_k/2)+\sin(3\theta_k/2)], \tag{4}$$

where $\tilde{r}_k = r_k/d$, and r_k and θ_k are the coordinates of the kth disclination (k=1, 2, 3) and $-\pi<\theta_k\le\pi$. For the disclination quadrupole shown in Fig. 2 and α in the range $-\pi<\alpha\le\pi$, we have $\tilde{r}_1=1$, $\tilde{r}_2=\sqrt{t^2+1}$, $\tilde{r}_3=t$; $\theta_1=\alpha+\pi/2-2\pi\ \Xi(\alpha-\pi/2)$, $\theta_2=\alpha+\mathrm{arccot}t-2\pi\Xi(\alpha+\mathrm{arccot}t-\pi)$, $\theta_3=\alpha$, where $\Xi(x)$ is the Heaviside function equal to unity for $x>0$ and zero otherwise.

In our model, the disclination strength ω, appearing in formulae (4), is arbitrary. In equilibrium, however, the disclination strength ω corresponds to the minimum of the energy change ΔW associated with the formation of the disclination quadrupole (Fig. 1). In the examined situation, the energy change ΔW can be presented as

$$\Delta W = W^q + W^{q-\sigma}. \tag{5}$$

Here, W^q is the proper energy of the disclination quadrupole, and $W^{q-\sigma}$ is the energy of its interaction with the stress field induced in the solid with a crack by the applied load σ_0.

The energy W^q of a disclination quadrupole near the tip of a long crack is calculated in the appendix as $W^q=D\omega^2d^2\,h(\alpha,t)/2$, where $D=G/[2\pi(1-\nu)]$, and $h(\alpha,t)$ is determined by formulae (A3)–(A6), (A8) and (A9).

The energy $W^{q-\sigma}$ can be written as (Romanov and Vladimirov, 1992)

$$W^{q-\sigma} = -\omega\int_S \sigma_{xy}dS, \tag{6}$$

where S is the area bounded by disclination quadrupole (i.e., the area of the plastically deformed grain), S' is the integration parameter and σ_{xy} is the component of the stress field created by the applied load σ_0 in a solid with a crack in the coordinate system (x, y) (see Fig. 2).

The stress σ_{xy} is obtained from the expressions (e.g., Panasyuk, 1988) for the stresses created by an applied tensile load in the vicinity of a crack tip as follows:

$$\sigma_{xy} = \frac{K_I^\sigma}{2\sqrt{2\pi r}}\sin\theta\cos\left(\frac{3\theta}{2}-2\alpha\right), \quad -\pi<\theta\le\pi. \tag{7}$$

Substitution of Eq. (7) to Eq. (6) yields: $W^{q-\sigma} = -K_I^\sigma\omega\, d^{3/2}\, f(\alpha,t)/(3\sqrt{2\pi})$, where

$$f(\alpha,t) = \begin{cases} g_1(\theta,\alpha)|_{\theta=\mathrm{arccot}t}^{\pi/2} + t^{3/2}g_2(\theta,\alpha)|_{\theta=0}^{\mathrm{arccot}t}, & -\pi<\alpha\le\pi/2, \\ g_1(\theta,\alpha)|_{\theta=\mathrm{arccot}t}^{\pi-\alpha} - g_1(\theta,\alpha)|_{\theta=\pi-\alpha}^{\pi/2} + t^{3/2}g_2(\theta,\alpha)|_{\theta=0}^{\mathrm{arccot}t}, & \pi/2<\alpha\le\pi-\mathrm{arccot}t, \\ -g_1(\theta,\alpha)|_{\theta=\mathrm{arccot}t}^{\pi/2} + t^{3/2}(g_2(\theta,\alpha)|_{\theta=0}^{\pi-\alpha} - g_2(\theta,\alpha)|_{\theta=\pi-\alpha}^{\mathrm{arccot}t}), & \pi-\mathrm{arccot}t<\alpha\le\pi, \end{cases} \tag{8}$$

$$g_1(\theta,\alpha) = \frac{4\cos^2[(\theta+\alpha)/2]\sin[(\theta-\alpha)/2]}{\sqrt{\sin\theta}}, \tag{9}$$

$$g_2(\theta,\alpha) = -\frac{4\cos^2[(\theta+\alpha)/2]\cos[(\theta-\alpha)/2]}{\sqrt{\cos\theta}}. \tag{10}$$

Now, the equilibrium disclination strength ω_0 that corresponds to the minimum of the energy change ΔW can be found from the relation $\partial\Delta W/\partial\omega|_{\omega=\omega_0}=0$, formula (5), and the above expressions for W^q and $W^{q-\sigma}$ as

$$\omega_0 = \frac{\sqrt{2\pi}(1-\nu)f(\alpha,t)K_I^\sigma}{3G\sqrt{d}h(\alpha,t)}. \tag{11}$$

Now, let us calculate the stress intensity factors k_I^q and k_{II}^q in the case of an equilibrium disclination quadrupole (characterized by $\omega=\omega_0$). Substitution of both the latter relation and formula (11) to the expressions for k_I^q and k_{II}^q yields $k_I^q = A\,K_I^\sigma$, $\quad k_{II}^q = B\,K_I^\sigma$, where

$$A = \frac{f(\alpha,t)f_1(\alpha,t)}{6h(a,t)}, \quad B = \frac{f(\alpha,t)f_2(\alpha,t)}{6h(\alpha,t)}. \tag{12}$$

After insertion of the latter relations for k_I^q and k_{II}^q to formula (3), we find the following solution of the resulting equation for K_{IC}:

$$K_{IC} = \frac{K_{IC}^\sigma}{\sqrt{(1+A)^2+B^2}}. \tag{13}$$

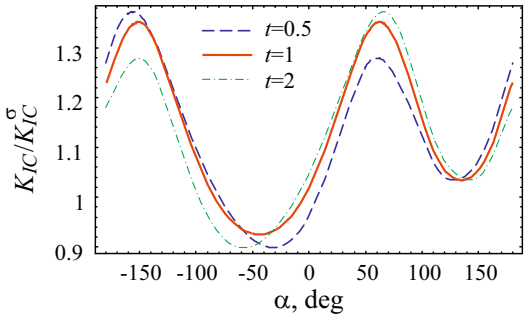

Fig. 3. Dependences of the normalized fracture toughness K_{IC}/K_{IC}^{σ} on the angle α, characterizing the orientation of the deformed grain near the crack tip, for various values of the ratio t of the sizes of grain facets.

Now, let us estimate the maximum value of ω_0 in the case of nanocrystalline Ni, Al and 3C-SiC. The maximum value of ω_0 corresponds to the crack with a critical length characterized by $K_I^{\sigma}=K_{IC}$ and can be calculated using the latter relation and formulae (11)–(13). For nanocrystalline Ni, we use the following parameter values (Smithells and Brand, 1976; Hirth and Lothe, 1982): G=73 GPa, ν=0.31, γ=1.725 J/m^2 and γ_b=0.69 J/m^2. Then, in the situation with $s=d$=15 nm and α=60°, we obtain: $\omega_0\approx 4^\circ$ $\omega_0\approx 4^\circ$, for a crack propagating inside a grain, and $\omega_0\approx 3.6^\circ$, for a crack that advances along a grain boundary. For nanocrystalline Al with G=27 GPa, ν=0.34, γ=0.56 and $\gamma_b=\gamma/2$, for $s=d$=15 nm and α=60°, we obtain $\omega_0\approx 3.9^\circ$, for a crack propagating inside a grain, and $\omega_0\approx 3.3^\circ$, for a crack that advances along a grain boundary.

In the case of nanocrystalline ceramic 3C-SiC materials characterized by G=217 GPa, ν=0.23, γ=1.84 (Ding et al., 2004) and $\gamma_b=\gamma/2$, for $s=d$=15 nm and α=60°, we have $\omega_0\approx 2.7^\circ$, for a crack propagating inside a grain, and $\omega_0\approx 2.3^\circ$, for a crack that advances along a grain boundary.

Formula (13) shows that the special rotational deformation increases the critical stress intensity factor (i.e., $K_{IC}>K_{IC}^{\sigma}$) if $-2<A<0$ and $|B|<\sqrt{-A\,(A+2)}$. Also, from formula (11) it follows that the quantities A and B depend only on the angle α (characterizing the quadrupole orientation) and the ratio $t=s/d$ of the sizes of grain facets. As a consequence, the normalized critical stress intensity factor K_{IC}/K_{IC}^{σ} (given by formula (13)) also depends only on α and t. The dependences of K_{IC}/K_{IC}^{σ} on the angle α are presented in Fig. 3, for various values of t. Fig. 3 shows that the special rotational deformation can either increase or decrease K_{IC}, depending on the value of the angle α, but, on average, increases it.

In the following, we assume that fracture in the examined nanocrystalline solid occurs through multiple crack propagation, which is affected by the formation of numerous disclination quadrupoles near crack tips. Taking into account the short-range character of the stress field of disclination quadrupoles, we also suppose that crack propagation is affected only by the rotational deformation of grains adjacent to crack tips. In this case, as a first approximation, the fracture toughness of the nanocrystalline solid can be defined as the average value of K_{IC} over various grain aspect ratios t and orientations α. Assuming that the angle α is random, we introduce a distribution in α described by the distribution function $\rho_\alpha(\alpha)=1/(2\pi)$, $-\pi<\alpha\leq\pi$. Also, we suppose that the grain aspect ratio t obeys the log-normal distribution $\rho_t(t)$ with the zero average value ($\overline{\ln t}=0$) and a dispersion s_0^2

$$\rho_t(t)=\frac{1}{t\sqrt{2\pi s_0^2}}\exp\left[-\ln^2 t/(2s_0^2)\right]. \tag{14}$$

In this case, the fracture toughness $\overline{K_{IC}}$ is given by

$$\overline{K_{IC}}=\int_{-\pi}^{\pi}\rho_a(\alpha)d\alpha\int_0^{\infty}K_{IC}(\alpha,t)\rho_t(t)dt=\frac{1}{2\pi\sqrt{2\pi s_0^2}}\int_{-\pi}^{\pi}d\alpha\int_0^{\infty}K_{IC}(\alpha,t)\,\frac{\exp[-\ln^2 t/(2s_0^2)]}{t}\,dt. \tag{15}$$

From formula (15) and the expressions for K_{IC}, we obtain $\overline{K_{IC}}/K_{IC}^{\sigma}\approx 1.13$, 1.12 and 1.10, for s_0=0, 0.5 and 1, respectively. Thus, the increase in fracture toughness due to special rotational deformation is around 10–15%.

3. Concluding remarks

Thus, we have theoretically described the effects of the special rotational deformation on growth of comparatively large cracks in deformed nanocrystalline ceramics and metals. The special rotational deformation is shown to relieve local stresses near the tips of comparatively large cracks in brittle nanocrystalline metals with finest grains and nanoceramics with widely ranged grains. It has been found that the special rotational deformation in these materials can increase the critical crack length (defined as the minimum length at which athermal propagation of a crack is energetically beneficial). In this context, the special rotational deformation can serve as a special toughening mechanism in nanocrystalline ceramics with widely ranged grain sizes and nanocrystalline metals with finest grains. Its effective action in nanocrystalline materials is due to the two following factors: (i) nanocrystalline materials are characterized by large volume fractions occupied by grain boundaries, and (ii) plastic deformation occurs at very high stresses in these materials. At the same time, the special rotational deformation hardly contributes to toughening of coarse-grained

polycrystalline metals, where the toughening mechanisms associated with plastic flow are realized through conventional dislocation emission from crack tips (see e.g., Rice and Thompson, 1974; Rice, 1992; Beltz et al., 1999). Besides, the rate of the special rotational deformation is controlled by diffusion providing grain boundary dislocation climb that accommodates grain boundary sliding (Ovid'ko and Sheinerman, 2008) (Fig. 1f–i). In a similar situation with grain rotations controlled by diffusion and driven by the sensitivity of the energy of a grain boundary to its misorientation parameters (Moldovan et al., 2001), the rate of grain rotations in nanocrystalline materials is by several orders larger than that in coarse-grained polycrystals. This is related to the fact that diffusion is highly accelerated with decreasing the grain size in a material due to corresponding increase in the volume fraction occupied by grain boundaries having enhanced diffusivity. Therefore, as with grain rotations (Moldovan et al., 2001), diffusion-controlled processes of special rotational deformation in nanocrystalline materials are highly enhanced and thereby much more typical, compared to those in coarse-grained polycrystals. In the context discussed, the special rotational deformation is expected to significantly contribute to stress relaxation near crack tips precisely in nanocrystalline materials, and is hardly effective in coarse-grained polycrystals.

With our theoretical results, the special rotational deformation can significantly contribute to the experimentally detected (Bhaduri and Bhaduri, 1997; Mirshams et al., 2001; Zhao et al., 2004; Kaminskii et al., 2005; Pei et al., 2005) enhancement of fracture toughness in nanocrystalline ceramics and metals. At the same time, in many other cases, fracture toughness of nanocrystalline materials is lower than that of their coarse-grained counterparts (see e.g., Kuntz et al., 2004; Koch et al., 2007). The discussed difference in fracture behavior between nanocrystalline materials is well illustrated by experimental data (Mirshams et al., 2001) concerning crack growth in nanocrystalline Ni specimens (with grain size around 20 nm) processed at different conditions. More precisely, Mirshams et al. (2001) reported that the crack growth resistance of nanocrystalline nickel thin sheets, in the cases of as-fabricated specimens and specimens after annealing at 373 K, exceeds the resistance of coarse-grained polycrystalline nickel. In contrast, after annealing at 473 K, nanocrystalline Ni shows low crack growth resistance, compared to that of coarse-grained Ni. These interesting experimental data are naturally explained in terms of the sensitivity of the special rotational deformation to the structure of grain boundaries. Such boundaries in the as-fabricated nanocrystalline metallic specimens are commonly non-equilibrium (Valiev, 2004; Ovid'ko, 2005; Koch et al., 2007). They contain many excess point and line defects, in which case intergrain sliding and climb of grain boundary dislocations along non-equilibrium grain boundaries in the as-fabricated nanocrystalline Ni specimens are enhanced. Annealing at comparatively low temperature, 373 K, does not dramatically change the non-equilibrium grain boundary structures. Therefore, the special rotational deformation conducted by both intergrain sliding and climb of grain boundary dislocations (Fig. 2) is enhanced and effectively hampers crack growth in the as-fabricated nanocrystalline Ni specimens and specimens after annealing at 373 K. In contrast, after annealing at 473 K, non-equilibrium grain boundaries transform into equilibrium ones. This is because 473 K is close to the characteristic temperature T_{GBD} at which intensive grain boundary diffusion processes occur and cause annihilation of extra defects at grain boundaries. (For metals, T_{GBD} is around $0.3T_m$, where T_m is the melting temperature (Vladimirov, 1975). For Ni, T_m=1728 K and T_{GBD} is around 520 K.) In these circumstances, the special rotational deformation is suppressed and hardly hampers crack growth in nanocrystalline Ni specimens after annealing at 473 K.

Finally, following numerous experiments, computer simulations and theoretical models [see e.g., reviews by Ovid'ko (2005), Wolf et al. (2005), Dao et al. (2005), Mukhopadhyay and Basu (2007)], several deformation mechanisms – lattice dislocation slip, grain boundary sliding, grain boundary diffusional creep, rotational deformation modes and others – can contribute to plastic flow processes in nanocrystalline materials. The role of each mechanism in plastic flow and its effect on fracture toughness of a nanocrystalline specimen crucially depends on structural and material parameters of the specimen as well as on the conditions of its mechanical loading. In general, different deformation/toughening mechanisms dominate in different nanocrystalline specimens. In the context discussed, our theoretical model of the special rotational deformation as a toughening mechanism can be viewed as part of the general theory of deformation mechanisms operating near crack tips and their contributions to toughening in nanocrystalline materials.

Acknowledgements

The work was supported, in part, by the Russian Foundation of Basic Research (Grant 08-01-00225-a), the Aristotle University of Thessaloniki (Subcontract of the Contract HPRN-CT-2002-00198), the National Science Foundation (Grant CMMI #0700272), Russian Academy of Sciences Program "Fundamental studies in nanotechnologies and nanomaterials," and the Russian Federal Agency of Science and Innovations (Grant MK-1702.2008.1).

Appendix

In this appendix, we calculate the stress field and energy of a disclination quadrupole near a crack tip (see Fig. 2). To do so, first, we calculate the stresses and energy of an individual wedge disclination of strength ω in a solid with a semi-infinite crack (Fig. A1). Let us introduce a Cartesian coordinate system (x, y) and a polar coordinate system (r, θ)

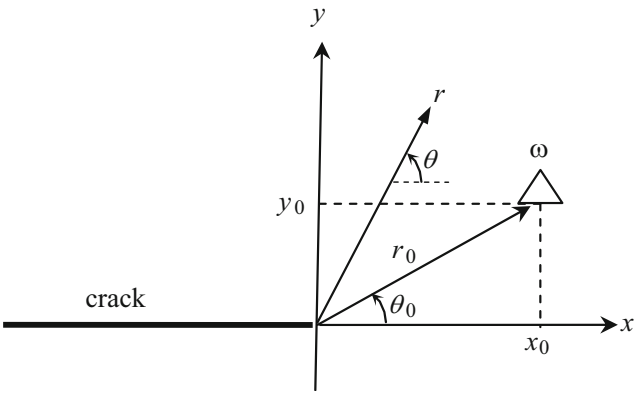

Fig. A1. Wedge disclination in a medium with a semi-infinite crack.

with the origins at the crack tip (Fig. A1). In this coordinate system, the disclination has the coordinates (x_0, y_0) and (r_0, θ_0), respectively. The stress field of the disclination can be presented in terms of complex functions Φ and Ω as (Stevenson, 1945)

$$\sigma_{xx}+\sigma_{yy}=4\mathrm{Re}\,\Phi(z), \tag{A1}$$

$$\sigma_{yy}-i\sigma_{xy}=\Phi(z)+\overline{\Omega(z)}+(z-\bar{z})\overline{\Phi'(z)}, \tag{A2}$$

where $i=\sqrt{-1}$, $z=x+iy=re^{i\theta}$ is the complex coordinate, and the overbar denotes the complex conjugate. The complex functions Φ and Ω associated with a wedge disclination in a solid with a flat semi-infinite crack are obtained from the known complex functions for an edge dislocation in a similar solid (Lin and Thomson, 1986; Ovid'ko and Sheinerman, 2009) through the representation of a wedge disclination as a continuous distribution of edge dislocation occupying the line between the crack tip and the position of the disclination. As a result, we have calculated the complex functions Φ and Ω for a disclination in a solid in a flat semi-infinite crack to be as follows:

$$\Phi(z)=\frac{D\omega}{2}\left\{\ln\left(\sqrt{z}-\sqrt{z_0}\right)-\ln\left(\sqrt{z}+\sqrt{\overline{z_0}}\right)+\frac{\sqrt{z_0}+\sqrt{\overline{z_0}}}{\sqrt{z}}+\frac{z_0-\overline{z_0}}{2\sqrt{z}\left(\sqrt{z}+\sqrt{\overline{z_0}}\right)}\right\}, \tag{A3}$$

$$\Omega(z)=\frac{D\omega}{2}\left\{\ln\left(\sqrt{z}-\sqrt{z_0}\right)-\ln\left(\sqrt{z}+\sqrt{\overline{z_0}}\right)+\frac{\sqrt{z_0}+\sqrt{\overline{z_0}}}{\sqrt{z}}+\frac{z_0-\overline{z_0}}{2\sqrt{z}\left(\sqrt{z}-\sqrt{z_0}\right)}\right\}, \tag{A4}$$

where $z_0=x_0+iy_0=r_0e^{i\theta}$, $D=G/[2\pi(1-\nu)]$, G is the shear modulus, and ν is Poisson's ratio.

Now, the stresses σ_{xx}, σ_{yy} and σ_{xy} follow from formula (A3) and the relations $\sigma_{xx}=\mathrm{Re}[4\Phi-g]$, $\sigma_{yy}=\mathrm{Re}g$, $\sigma_{xy}=-\mathrm{Im}g$, where $g=\Phi+\overline{\Omega}+(z-\bar{z})\,\overline{\Phi}'$. We have verified that these stresses satisfy the equations of equilibrium and free-traction conditions at the crack surface and tend to zero as the distance from the disclination tends to infinity.

The self-energy of the disclination shown in Fig. A1 is given (Romanov and Vladimirov, 1992) by

$$W^{\triangle}(r_0,\theta_0)=\frac{\omega}{2}\int_0^{r_0}\sigma_{\theta\theta}(r,r_0,\theta,\theta_0)|_{\theta=\theta_0}(r_0-r)dr, \tag{A5}$$

where $\sigma_{\theta\theta}$ is the component of the disclination stress field in the cylindrical coordinate system,

$$\sigma_{\theta\theta}(r,r_0,\theta,\theta_0)=\sigma_{xx}\sin^2\theta+\sigma_{yy}\cos^2\theta-\sigma_{xy}\sin 2\theta=4\mathrm{Re}\,\Phi\sin^2\theta+\mathrm{Re}g\cos 2\theta+\mathrm{Im}g\sin 2\theta \tag{A6}$$

Substitution of (A3), (A4) and (A6) to (A5) and numerical integration yields

$$W^{\triangle}=\frac{D\omega^2r_0^2}{2}F(\theta_0), \tag{A7}$$

where the function $F(\theta_0)$ is depicted in Fig. A2. The maximum self-energy $W_m^{\triangle}$ of a disclination located at a specified distance r_0 from the crack tip is reached at $\theta_0=0$ and follows as $W_m^{\triangle}=D\omega^2r_0^2$. At $\theta_0\to 0$, when the disclination approaches the surface of the solid, its energy tends to zero.

By setting $r_0=H/\sin\theta$, assuming H to be independent of θ and coming to the limit of $\theta_0\to\pi$, one can come to the known case of a disclination in a semi-infinite solid, located at a distance H from its flat surface. In this case, the energy $W_{hs}^{\triangle}$ of a disclination in a half-space is calculated as $W_{hs}^{\triangle}=D\omega^2H^2\lim\limits_{\theta_0\to\pi}F(\theta_0)/(2\sin^2\theta_0)$. Numerical evaluation shows that $\lim\limits_{\theta_0\to\pi}F(\theta_0)/(2\sin^2\theta_0)=1/2$, and so $W_{hs}^{\triangle}=D\omega^2H^2/2$, which coincides with the known result (Romanov and Vladimirov, 1992).

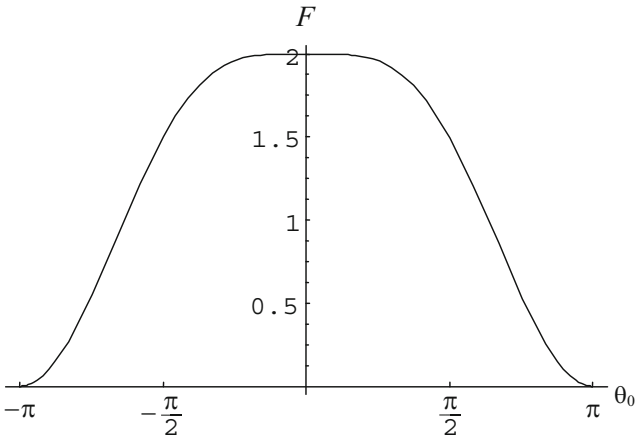

Fig. A2. Function $F(\theta_0)$ characterizing the dependence of the energy of a wedge disclination in a solid with a semi-infinite crack (in units of $D\omega^2 r_0^2/2$) on the angular disclination coordinate θ_0.

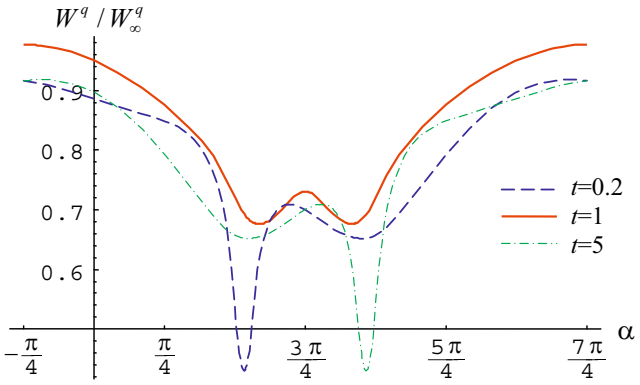

Fig. A3. Ratio W^q/W^q_∞ of the energy W^q of a disclination quadrupole near a crack tip to the energy W^q_∞ of a similar quadrupole in an infinite uncracked solid, as a function of the angle α, for various values of the quadrupole aspect ratio t.

The expressions for the stresses and energy of a disclination in a solid with a crack allow one to calculate the energy W^q of the disclination quadrupole shown in Fig. 2 (which transforms to three disclinations in the examined case of a semi-infinite crack). The energy of the disclination quadrupole is presented as

$$W^q = W^{\triangle}(r_1,\theta_1)+W^{\triangle}(r_2,\theta_2)+W^{\triangle}(r_3,\theta_3)-W_{\rm int}(r_1,r_2,\theta_1,\theta_2)+W_{\rm int}(r_1,r_3,\theta_1,\theta_3)-W_{\rm int}(r_2,r_3,\theta_2,\theta_3). \tag{A8}$$

In formula (A8), (r_k,θ_k) (k=1, 2, 3) are the coordinates of the three disclinations given above in the main text, and $W_{int}(r_j,r_k,\theta_j,\theta_k)$ (j,k=1, 2, 3) denotes the energy of the interaction between two disclinations of strength, ω, with the coordinates $(r_j,\ \theta_j)$ and $(r_k,\ \theta_k)$. The energy $W_{int}(r_j,r_k,\theta_j,\theta_k)$ follows as (Romanov and Vladimirov, 1992)

$$W_{int}(r_j,r_k,\theta_j,\theta_k) = \omega\int_0^{r_k}\sigma_{\theta\theta}(r,r_j,\theta,\theta_j)\big|_{\theta=\theta_k}(r_k-r)dr. \tag{A9}$$

Insertion of formulae (A3)–(A6) and (A9) to Eq. (A8) yields $W^q=(D\omega^2d^2/2)\,h(\alpha,t)$, where $t=s/d$ and the function $h(\alpha,t)$ is evaluated numerically.

Let us compare the energy W^q of the disclination quadrupole near a crack tip with the energy W^q_∞ of a similar quadrupole in an infinite solid without cracks. The energy W^q_∞ is given by (Romanov and Vladimirov, 1992; Gutkin et al., 2002b)

$$W^q_\infty = \frac{D\omega^2d^2}{2}\{(1+t^2)\ln(1+t^2)-t^2\ln(t^2)\}. \tag{A10}$$

The ratio W^q/W^q_∞ as a function of the angle α is plotted in Fig. A3, for various values of the quadrupole aspect ratio t. As is seen in Fig. A3, for t in the range from 0.2 to 5, the presence of the crack reduces the disclination quadrupole energy by 2–42%.

References

Aifantis, E.C., 2000. Nanomechanics: an Introduction. In: Katsikadelis, T., Beskos, D.E., Gdoutos, E.E. (Eds.), Recent Advances in Applied Mechanics (Honorary Volume for Academician A.N. Kounadis). National Technical University of Athens, Athens, pp. 243–254.

Aifantis, E.C., 2009. Deformation and failure of bulk nanograined and UFG materials. Mater. Sci. Eng. A 503, 190–201.

Aifantis, K.E., Ngan, A.H.W., 2007. Modeling dislocation–grain boundary interactions through gradient plasticity and nanoindentation. Mater. Sci. Eng. A 459, 251–261.

Aifantis, K.E., Soer, W.A., De Hosson, J.T.M., 2005. Incipient plasticity during nanoindentation at grain boundaries in body-centered cubic metals. Acta Mater. 53, 4665–4676.

Aifantis, K.E., Soer, W.A., De Hosson, J.T.M., Willis, J.R., 2006. Interfaces within strain gradient plasticity: theory and experiments. Acta Mater. 54, 5077–5085.

Ashby, M.F., Verall, R.A., 1973. Diffusion-accommodated flow and superplasticity. Acta Metall. 21, 149–163.

Barai, P., Weng, G.J., 2008a. Mechanics of creep resistance in nanocrystalline solids. Acta Mech. 195, 327–348.

Barai, P., Weng, G.J., 2008b. The competition of grain size and porosity in the viscoplastic response of nanocrystalline solids. Int. J. Plasticity 24, 1380–1410.

Beltz, G.E., Lipkin, D.M., Fischer, L.L., 1999. Role of crack blunting in ductile versus brittle response of crystalline materials. Phys. Rev. Lett. 82, 4468–4471.

Bhaduri, S., Bhaduri, S.B., 1997. Enhanced low temperature toughness of Al_2O_3–ZrO_2 nano/nano composites. Nanostruct. Mater. 8, 755–763.

Bobylev, S.V., Gutkin, M.Y.u, Ovid'ko, I.A., 2006. Partial and split dislocation configurations in nanocrystalline metals. Phys. Rev. B 73, 064102.

Bobylev, S.V., Mukherjee, A.K., Ovid'ko, I.A., 2009a. Transition from plastic shear into rotation deformation mode in nanocrystalline metals and ceramics. Rev. Adv. Mater. Sci. 19, 103–113.

Bobylev, S.V., Mukherjee, A.K., Ovid'ko, I.A., 2009b. Emission of partial dislocations from amorphous intergranular boundaries in deformed nanocrystalline ceramics. Scr. Mater. 60, 36–39.

Capolungo, L., Spearot, D.E., Cherkaoui, M., McDowell, D.L., Qu, J., Jacob, K.I., 2007. Dislocation nucleation from bicrystal interfaces and grain boundary ledges: relationship to nanocrystalline deformation. J. Mech. Phys. Solids 55, 2300–2327.

Chen, M.W., Ma, E., Hemker, K.J., Sheng, H.W., Wang, Y.M., Cheng, X.M., 2003. Deformation twinning in nanocrystalline aluminum. Science 300, 1275–1277.

Choi, I.S., Detor, A.J., Schwaiger, R., Dao, M., Schuh, C.A., Suresh, S., 2008. Mechanics of indentation of plastically graded materials—II: experiments on nanocrystalline alloys with grain size gradients. J. Mech. Phys. Solids 56, 172–183.

Conrad, H., Narayan, J., 2000. On the grain size softening in nanocrystalline materials. Scr. Mater. 42, 1025–1030.

Dao, M., Lu, L., Asaro, R.J., De Hosson, J.T.M., Ma, E., 2005. Toward a quantitative understanding of mechanical behavior of nanocrystalline metals. Acta Mater. 55, 4041–4065.

Demkowicz, M.J., Argon, A.S., Farkas, D., Frary, M., 2007. Simulation of plasticity in nanocrystalline silicon. Philos. Mag. 87, 4253–4271.

Ding, Z., Zhou, S., Zhao, Y., 2004. Hardness and fracture toughness of brittle materials: a density functional theory study. Phys. Rev. B 70, 184117.

De Hosson, J.T.M., Soer, W.A., Minor, A.M., Shan, Z., Stach, E.A., Syed Asif, S.A., Warren, O.L., 2006. In situ TEM nanoindentation and dislocation–grain boundary interactions: a tribute to David Brandon. J. Mater. Sci. 41, 7704–7719.

Gurtin, M.E., Anand, L., 2008. Nanocrystalline grain boundaries that slip and separate: a gradient theory that accounts for grain-boundary stress and conditions at a triple-junction. J. Mech. Phys. Solids 56, 184–199.

Gutkin, M.Y.u, Kolesnikova, A.L., Ovid'ko, I.A., Skiba, N.V., 2002a. Disclinations and rotational deformation in fine-grained materials. Philos. Mag. Lett. 82, 651–657.

Gutkin, M.Y.u, Mikaelyan, K.N., Romanov, A.E., Klimanek, P., 2002b. Disclination models of misorientation band generation and propagation. Phys. Status Solidi (a) 193, 35–52.

Gutkin, M.Y.u, Ovid'ko, I.A., 2004. Plastic Deformation in Nanocrystalline Materials. Springer, Berlin, New York etc.

Gutkin, M.Y.u, Ovid'ko, I.A., 2005. Grain boundary migration as rotational deformation mode in nanocrystalline materials. Appl. Phys. Lett. 87, 251916.

Gutkin, M.Y.u, Ovid'ko, I.A., Skiba, N.V., 2003. Crossover from grain boundary sliding to rotational deformation in nanocrystalline materials. Acta Mater. 51, 4059–4071.

Gutkin, M.Y.u, Ovid'ko, I.A., Skiba, N.V., 2008. Crack-stimulated generation of deformation twins in nanocrystalline metals and ceramics. Philos. Mag. 88, 1137–1151.

Hackney, S., Ke, M., Milligan, W.W., Aifantis, E.C., 1996. Grain size and strain rate effects on the mechanisms of deformation and fracture in nanostructured metals. In: Suryanarayana, C. (Ed.), Processing and Properties of Nanocrystalline Materials. TMS, Warrendale, PA, pp. 421–426.

Hirth, J.P., Lothe, J., 1982. Theory of Dislocations. Wiley, New York.

Irwin, R.G., 1957. Analysis of stresses and strains near the end of a crack traversing a plate. J. Appl. Mech. 24, 361–364.

Jin, M., Minor, A.M., Stach, E.A., Morris Jr., J.W., 2004. Direct observation of deformation-induced grain growth during the nanoindentation of ultrafine-grained Al at room temperature. Acta Mater. 52, 5381–5387.

Joshi, S.P., Ramesh, K.T., 2008. Stability map for nanocrystalline and amorphous materials. Phys. Rev. Lett. 101, 025501.

Kaminskii, A.A., Akchurin, M.S.h, Gainutdinov, R.V., Takaichi, K., Shirakava, A., Yagi, H., Yanagitani, T., Ueda, K., 2005. Microhardness and fracture toughness of Y_2O_3- and $Y_3Al_5O_{12}$-based nanocrystalline laser ceramics. Crystallogr. Rep. 50, 869–873.

Ke, M., Milligan, W.W., Hackney, S.A., Carsley, J.E., Aifantis, E.C., 1995. Observation and measurement of grain rotation and plastic strain in nanostructured metal thin films. Nanostruct. Mater. 5, 689–697.

Koch, C.C., Ovid'ko, I.A., Seal, S., Veprek, S., 2007. In: Structural Nanocrystalline Materials: Fundamentals and Applications. Cambridge University Press, Cambridge.

Kuntz, J.D., Zhan, G.-D., Mukherjee, A.K., 2004. Nanocrystalline-matrix ceramic composites for improved fracture toughness. MRS Bull. 29, 22–27.

Latapie, A., Farkas, D., 2004. Molecular dynamics investigation of the fracture behavior of nanocrystalline α-Fe. Phys. Rev. B 69, 134110.

Liao, X.Z., Zhou, F., Srinivasan, S.G., Zhu, Y.T., Valiev, R.Z., Gunderov, D.V., 2004. Deformation twinning in nanocrystalline copper at room temperature and low strain rate. Appl. Phys. Lett. 84, 592–594.

Lin, I.-H., Thomson, R., 1986. Cleavage, dislocation emission, and shielding for cracks under general loading. Acta Metall. 34, 187–206.

Liu, H., Huang, C., Teng, X., Wang, H., 2008. Effect of special microstructure on the mechanical properties of nanocomposite. Mater. Sci. Eng. A 487, 258–263.

Milligan, W.W., Hackney, S.A., Ke, M., Aifantis, E.C., 1993. In situ studies of deformation and fracture in nanophase materials. Nanostruct. Mater. 2, 267–276.

Mirshams, R.A., Liao, C.H., Wang, S.H., Yin, W.M., 2001. R-curve characterization of the fracture toughness of nanocrystalline nickel thin sheets. Mater. Sci. Eng. A 315, 21–27.

Moldovan, D., Wolf, D., Phillpot, S.R., 2001. Theory of diffusion-accommodated grain rotation in columnar polycrystalline microstructures. Acta Mater. 49, 3521–3532.

Morozov, N.F., Ovid'ko, I.A., Petrov, Yu.V., Sheinerman, A.G., 2009. Generation and convergence of nanocracks in nanocrystalline materials deformed by grain boundary sliding. Rev. Adv. Mater. Sci. 19, 63–72.

Mukhopadhyay, A., Basu, B., 2007. Consolidation–microstructure–property relationships in bulk nanoceramics and ceramic nanocomposites: a review. Int. Mater. Rev. 52, 257–288.

Mukherjee, A.K., 2002. An examination of the constitutive equation for elevated temperature plasticity. Mater. Sci. Eng. A 322, 1–22.

Murayama, M., Howe, J.M., Hidaka, H., Takaki, S., 2002. Atomic-level observation of disclination dipoles in mechanically milled, nanocrystalline Fe. Science 295, 2433–2435.

Ovid'ko, I.A., 2002. Deformation of nanostructures. Science 295, 2386.
Ovid'ko, I.A., 2005. Deformation and diffusion modes in nanocrystalline materials. Int. Mater. Rev. 50, 65–82.
Ovid'ko, I.A., Sheinerman, A.G., 2008. Special rotational deformation in nanocrystalline metals and ceramics. Scr. Mater. 59, 119–122.
Ovid'ko, I.A., Sheinerman, A.G., 2009. Grain size effect on crack blunting in nanocrystalline materials. Scr. Mater. 60, 627–630.
Ovid'ko, I.A., Sheinerman, A.G., Aifantis, E.C., 2008. Stress-driven migration of grain boundaries and fracture processes in nanocrystalline ceramics and metals. Acta Mater. 56, 2718–2727.
Padmanabhan, K.A., Gleiter, H., 2004. Optimal structural superplasticity in metals and ceramics of microcrystalline- and nanocrystalline-grain sizes. Mater. Sci. Eng. A 381, 28–38.
Panasyuk, V.V. (Ed.), Naukova Dumka, vol. 2; 1988 (in Russian).
Pande, C.S., Cooper, K.P., 2009. Nanomechanics of Hall–Petch relationship in nanocrystalline materials. Prog. Mater. Sci. 54, 689–706.
Pande, C.S., Masumura, R.A., 2005. Grain growth and deformation in nanocrystalline materials. Mater. Sci. Eng. A 409, 125–130.
Pei, Y.T., Galvan, D., De Hosson, J.T.M., 2005. Nanostructure and properties of TiC/a-C:H composite coatings. Acta Mater. 53, 4505–4521.
Rice, J.R., 1992. Dislocation nucleation from a crack tip: an analysis based on the Peierls concept. J. Mech. Phys. Solids 40, 239–271.
Rice, J.R., Thompson, R.M., 1974. Ductile versus brittle behaviour of crystals. Philos. Mag. 29, 73–97.
Romanov, A.E., Vladimirov, V.I., 1992. Disclinations in crystalline solids. In: Nabarro, F.R.N. (Ed.), Dislocations in Solids, vol. 9. North-Holland Publ. Co., Amsterdam, pp. 191–302.
Shan, Zh., Stach, E.A., Wiezorek, J.M.K., Knapp, J.A., Follstaedt, D.M., Mao, S.X., 2004. Grain boundary-mediated plasticity in nanocrystalline nickel. Science 305, 654–657.
Shimokawa, T., Nakatani, A., Kitagawa, H., 2005. Grain-size dependence of the relationship between intergranular and intragranular deformation of nanocrystalline Al by molecular dynamics simulations. Phys. Rev. B 71, 224110.
Siegel, R.W., Chang, S.K., Ash, B.J., Stone, J., Ajayan, P.M., Doremus, R.W., Schadler, L.S., 2001. Mechanical behavior of polymer and ceramic matrix nanocomposites. Scr. Mater. 44, 2061–2064.
Smithells, C.J., Brands, E.A., 1976. In: Metals Reference Book. Butterworth, London.
Soer, W.A., De Hosson, J.T.M., Minor, A.M., Morris Jr., J.W., Stach, E.A., 2004. Effects of solute Mg on grain boundary and dislocation dynamics during nanoindentation of Al–Mg thin films. Acta Mater. 52, 5783–5790.
Stevenson, A.C., 1945. Complex potentials in two-dimensional elasticity. Proc. R. Soc. A 184, 129–179.
Szlufarska, I., Nakano, A., Vashista, P., 2005. A crossover in the mechanical response of nanocrystalline ceramics. Science 309, 911–914.
Tomar, V., Zhou, M., 2007. Analyses of tensile deformation of nanocrystalline α-Fe_2O_3+*fcc*-Al composites using molecular dynamics simulations. J. Mech. Phys. Solids 55, 1053–1085.
Valiev, R.Z., 2004. Nanostructuring of metals by severe plastic deformation for advanced properties. Nat. Mater. 3, 511–516.
Vladimirov, V.I., 1975. In: Einführung in die Physikalische Theorie der Plastizität und Festigkeit. VEB Deutscher Verlag für Grundstoffindustrie, Leipzig.
Wang, Y.M., Hodge, A.M., Biener, J., Hamza, A.V., Barnes, D.E., Liu, K., Nieh, T.G., 2005. Deformation twinning during nanoindentation of nanocrystalline Ta. Appl. Phys. Lett. 86, 101915.
Wei, Y., Anand, L., 2004. Grain-boundary sliding and separation in polycrystalline metals: application to nanocrystalline f.c.c. metals. J. Mech. Phys. Solids 52, 2587–2616.
Wei, Y., Gao, H., 2008. An elastic–viscoplastic model of deformation in nanocrystalline metals based on coupled mechanics in grain boundaries and grain interiors. Mater. Sci. Eng. A 478, 16–25.
Wei, Y., Bower, A.F., Gao, H., 2008. Enhanced strain-rate sensitivity in f.c.c. nanocrystals due to grain-boundary diffusion and sliding. Acta Mater. 56, 1741–1752.
Weng, G.J., 2009. A homogenization scheme for the plastic properties of nanocrystalline materials. Rev. Adv. Mater. Sci. 19, 41–62.
Wolf, D., Yamakov, V., Phillpot, S.R., Mukherjee, A.K., Gleiter, H., 2005. Deformation of nanocrystalline materials by molecular-dynamics simulation: relationship to experiments? Acta Mater 53, 1–40.
Yang, W., Wang, H.T., 2004. Mechanics modeling for deformation of nano-grained metals. J. Mech. Phys. Solids 52, 875–889.
Yang, F., Yang, W., 2008. Brittle versus ductile transition of nanocrystalline metals. Int. J. Solids Struct. 45, 3897–3907.
Yang, F., Yang, W., 2009. Crack growth versus blunting in nanocrystalline metals with extremely small grain size. J. Mech. Phys. Solids 57, 305–324.
Zhan, G.-D., Kuntz, J.D., Wan, J., Mukherjee, A.K., 2003. Single-wall carbon nanotubes as attractive toughening agents in alumina-based nanocomposites. Nat. Mater. 2, 38–42.
Zhang, T.-Y., Li, J.C.M., 1991. Cleavage, dislocation emission, and shielding for cracks under general loading. Acta Metall. Mater. 39, 2739–2744.
Zhang, K., Weertman, J.R., Eastman, J.A., 2004. The influence of time, temperature, and grain size on indentation creep in high-purity nanocrystalline and ultrafine grain copper. Appl. Phys. Lett. 85, 5197–5199.
Zhang, K., Weertman, J.R., Eastman, J.A., 2005. Rapid stress-driven grain coarsening in nanocrystalline Cu at ambient and cryogenic temperatures. Appl. Phys. Lett. 87, 061921.
Zhao, Y., Qian, J., Daemen, L.L., Pantea, C., Zhang, J., Voronin, G.A., Zerda, T.W., 2004. Enhancement of fracture toughness in nanostructured diamond–SiC composites. Appl. Phys. Lett. 84, 1356–1358.
Zizak, I., Gerlach, J.W., Assmann, W., 2008. Ion-beam-induced collective rotation of nanocrystals. Phys. Rev. Lett. 101, 065503.